HHS Public Access

Author manuscript

Neurobiol Learn Mem. Author manuscript; available in PMC 2018 December 01.

Published in final edited form as:

Neurobiol Learn Mem. 2017 December ; 146: 47–57. doi:10.1016/j.nlm.2017.11.004.

Persistent, generalized hypersensitivity of olfactory bulb interneurons after olfactory fear generalization

Marley D. Kass and **John P. McGann***

Behavioral & Systems Neuroscience Section, Department of Psychology, Rutgers, The State University of New Jersey, 152 Frelinghuysen Road, Piscataway, NJ 08854

Abstract

Generalization of fear from previously threatening stimuli to novel but related stimuli can be beneficial, but if fear overgeneralizes to inappropriate situations it can produce maladaptive behaviors and contribute to pathological anxiety. Appropriate fear learning can selectively facilitate early sensory processing of threat-predictive stimuli, but it is unknown if fear generalization has similarly generalized neurosensory consequences. We performed *in vivo* optical neurophysiology to visualize odor-evoked neural activity in populations of periglomerular interneurons in the olfactory bulb 1 day before, 1 day after, and 1 month after each mouse underwent an olfactory fear conditioning paradigm designed to promote generalized fear of odors. Behavioral and neurophysiological changes were assessed in response to a panel of odors that varied in similarity to the threat-predictive odor at each time point. After conditioning, all odors evoked similar levels of freezing behavior, regardless of similarity to the threat-predictive odor. Freezing significantly correlated with large changes in odor-evoked periglomerular cell activity, including a robust, generalized facilitation of the response to all odors, broadened odor tuning, and increased neural responses to lower odor concentrations. These generalized effects occurred within 24 hours of a single conditioning session, persisted for at least 1 month, and were detectable even in the first moments of the brain's response to odors. The finding that generalized fear includes altered early sensory processing of not only the threat-predictive stimulus but also novel though categorically-similar stimuli may have important implications for the etiology and treatment of anxiety disorders with sensory sequelae.

Keywords

Olfactory fear conditioning; Fear generalization; Anxiety disorders; Sensory plasticity; Olfactory bulb; Optical neurophysiology

*Corresponding author: John P. McGann, PhD, Department of Psychology, Rutgers University, 152 Frelinghuysen Road, Piscataway, NJ 08854 USA, john.mcgann@rutgers.edu, Phone: 617-519-7232.

Author Contributions

M.D.K designed the study, performed the optical neurophysiology and behavioral experiments, analyzed the data, and wrote the paper. J.P.M. analyzed the data and wrote the paper.

Competing Interests

The authors declare no financial or non-financial competing interests.

1. Introduction

Generalization of learned fear is an adaptive mechanism that promotes flexible responding to novel but potentially dangerous situations. Learned fear is studied through classical conditioning paradigms that pair a neutral sensory stimulus such as an odor (the conditioned stimulus, CS) with an aversive stimulus such as a shock (the unconditioned stimulus, US) that elicits an unconditioned defensive response. After conditioning, the defensive response will be elicited by the CS but will also generalize to non-threatening stimuli related to the CS (Dunsmoor, Mitroff, & LaBar, 2009; Dunsmoor, White, & LaBar, 2011b; Lissek, Biggs, Rabin, Cornwell, Alvarez, Pine et al., 2008; Rajbhandari, Zhu, Adling, Fanselow, & Waschek, 2016; Resnik & Paz, 2015; Resnik, Sobel, & Paz, 2011). Generalization of conditioned fear typically falls off gradually as stimuli become more dissimilar to the CS along continuous, physical axes, such as tone frequency (Aizenberg & Geffen, 2013; Resnik & Paz, 2015; Resnik et al., 2011) or geometric size (Lissek et al., 2008; Lissek, Kaczkurkin, Rabin, Geraci, Pine, & Grillon, 2014; Lissek, Rabin, Heller, Lukenbaugh, Geraci, Pine et al., 2010), though generalization also can occur within conceptual categories (Dunsmoor & Murphy, 2015; Dunsmoor et al., 2011b). Fear overgeneralization occurs when cues that do not actually predict dangerous outcomes evoke maladaptive fearful or defensive responses (van Meurs, Wiggert, Wicker, & Lissek, 2014). Patients with anxiety disorders exhibit broadened fear generalization compared to healthy controls (Lissek et al., 2014; Lissek et al., 2010), suggesting that overgeneralization of learned fear may contribute to the etiology or maintenance of pathological fear (Dunsmoor & Paz, 2015; Resnik & Paz, 2015).

Most research addressing the neurobiology of conditioned fear has focused on structures such as the amygdala, hippocampus, and prefrontal cortex (Dunsmoor & Paz, 2015; Jovanovic & Ressler, 2010; LeDoux, 2000; Maren & Quirk, 2004; Phelps & LeDoux, 2005). However, fear learning also induces dramatic changes in sensory regions (Bakin & Weinberger, 1990; Chen, Barnes, & Wilson, 2011; Fletcher, 2012; Gdalyahu, Tring, Polack, Gruver, Golshani, Fanselow et al., 2012; Li, Howard, Parrish, & Gottfried, 2008; McGann, 2015; Quirk, Armony, & LeDoux, 1997; Weinberger, 2007), including CS-specific hypersensitivity in primary sensory neurons (Dias & Ressler, 2014; Jones, Choi, Davis, & Ressler, 2008; Kass, Rosenthal, Pottackal, & McGann, 2013d). This plasticity can have explicitly sensory consequences, such as lowered detection thresholds (Ahs, Miller, Gordon, & Lundstrom, 2013; Parma, Ferraro, Miller, Ahs, & Lundstrom, 2015) or altered perceptual discrimination abilities (Aizenberg & Geffen, 2013; Chen et al., 2011; Fletcher & Wilson, 2002; Li et al., 2008; Resnik & Paz, 2015; Resnik et al., 2011), but it may also be important for non-sensory functions like recruiting attention or triggering defensive behavior (McGann, 2015). Fear generalization has been presumed to reflect changes in higher-order structures responding to sensory inputs (Ciocchi, Herry, Grenier, Wolff, Letzkus, Vlachos et al., 2010; Dunsmoor & Paz, 2015; Dunsmoor, Prince, Murty, Kragel, & LaBar, 2011a; Ghosh & Chattarji, 2015; Resnik & Paz, 2015), but sensory regions might be responsible for labeling CS-resembling stimuli as potentially threatening (Aizenberg & Geffen, 2013; Chen et al., 2011; Krusemark & Li, 2012; Miasnikov & Weinberger, 2012). Psychopathologies like post-traumatic stress disorder (PTSD) include alterations in attentional and neurosensory processing (Bryant, Felmingham, Kemp, Barton, Peduto, Rennie et al., 2005;

Clancy, Ding, Bernat, Schmidt, & Li, 2017; Mueller-Pfeiffer, Schick, Schulte-Vels, O'Gorman, Michels, Martin-Soelch et al., 2013; Olatunji, Armstrong, McHugo, & Zald, 2013; Todd, MacDonald, Sedge, Robertson, Jetly, Taylor et al., 2015) that might reflect dysfunctional plasticity in early sensory brain regions.

In the olfactory system, odors are initially processed in the olfactory bulb, where "bottom-up" sensory input from olfactory sensory neurons (OSNs) in the nose converges with "top-down" projections from structures involved in fear learning (Carmichael, Clugnet, & Price, 1994; de Olmos, Hardy, & Heimer, 1978; Shipley & Ennis, 1996; Zaborszky, Carlsen, Brashear, & Heimer, 1986). After olfactory fear conditioning, odor-evoked neural activity is enhanced in the olfactory bulb (Fletcher, 2012; Sevelinges, Moriceau, Holman, Miner, Muzny, Gervais et al., 2007), even as early as the synaptic terminals of OSNs (Kass et al., 2013d). To investigate whether fear generalization would alter bulbar processing, we focused on the physiology of inhibitory periglomerular (PG) interneurons, which shape the input and output of the olfactory bulb (McGann, 2013; McGann, Pirez, Gainey, Muratore, Elias, & Wachowiak, 2005; Murphy, Darcy, & Isaacson, 2005; Shao, Puche, Kiyokage, Szabo, & Shipley, 2009; Shao, Puche, Liu, & Shipley, 2012). PG interneurons integrate peripheral input from receptor-specific populations of OSNs with lateral information about other OSN populations (Aungst, Heyward, Puche, Karnup, Hayar, Szabo et al., 2003; Liu, Plachez, Shao, Puche, & Shipley, 2013) and also with top-down information from cortical and neuromodulatory structures (Boyd, Sturgill, Poo, & Isaacson, 2012; Eckmeier & Shea, 2014; Liu, Shao, Puche, Wachowiak, Rothermel, & Shipley, 2015; Ma & Luo, 2012; Markopoulos, Rokni, Gire, & Murthy, 2012; Shipley & Ennis, 1996). Notably, PG cell activity is influenced by interactions between the amygdala and locus coeruleus (LC) (Fast & McGann, 2017), which are both involved in emotional processes (Aston-Jones, Rajkowski, Kubiak, Valentino, & Shipley, 1996; LeDoux, 2000). Such modulation might enable PG cells to facilitate the detection of potentially threatening sensory cues.

2. Materials and Methods

2.1. Subjects

Experiments used a total of 66 adult (5.5±0.12 months) male mice in accordance with protocols approved by the Rutgers University IACUC. Mice used for optical neurophysiology expressed the genetically-encoded calcium indicators GCaMP3 (Zariwala, Borghuis, Hoogland, Madisen, Tian, De Zeeuw et al., 2012) (Jackson Laboratory, stock #014538) or GCaMP6f (Chen, Wardill, Sun, Pulver, Renninger, Baohan et al., 2013) (Jackson Laboratory, stock #024105) via cre recombinase-mediated recombination in cells expressing the *gad2* gene (Taniguchi, He, Wu, Kim, Paik, Sugino et al., 2011) (Jackson Laboratory, stock #010802), which includes PG interneurons in the olfactory bulb (Fast & McGann, 2017; Wachowiak, Economo, Diaz-Quesada, Brunert, Wesson, White et al., 2013). These mice are on mixed backgrounds, though mostly C57BL/6 (per Jackson Laboratory development details). Purely behavioral experiments used wild-type C57BL/6J mice (Jackson Laboratory, stock #000664) and *gad2-cre*$^{-/+}$×GCaMP$^{-/-}$ littermates.

2.2. Olfactory Fear Conditioning

Subjects underwent random group assignment followed by 2 15-min context pre-exposures (to minimize shock-context associations), 1 day of training, and repeated post-training behavioral tests in a novel context (Figure 1A). To promote fear generalization (Aizenberg & Geffen, 2013; Baldi, Lorenzini, & Bucherelli, 2004; Chen et al., 2011; Fanselow, 1980; Ghosh & Chattarji, 2015; Laxmi, Stork, & Pape, 2003; Poulos, Mehta, Lu, Amir, Livingston, Santarelli et al., 2016; Shaban, Humeau, Herry, Cassasus, Shigemoto, Ciocchi et al., 2006), paired training included 10 trials of an ~15-sec ester-odor (methyl valerate, MV) that approximately coterminated with a strong 1.2-mA, 0.5-sec footshock (Figure 1B–C). Shock-alone and odor-alone control training consisted of the same paradigm, but *without* the presentation of any odors (Figure 1B, middle) or any shocks (Figure 1B, bottom), respectively. Training sessions began with a 180-sec acclimation period and employed long, variable inter-trial intervals (ITIs; 228–348 sec). Note that each conditioning chamber was equipped with its own custom-built olfactometer and was modified to contain a port for odor delivery and a vacuum exhaust for odor removal. All odors were diluted in mineral oil and were presented at a flow rate of ~1.0–1.2 sL/min. Olfactometer calibrations were performed via photoionization detection measurements (ppbRAE 3000) to ensure reliable odor concentrations (reported in arbitrary units, au), across trials, sessions, and chambers. The dilution of the odor in the jar and the air flow rate were adjusted as needed to yield MV concentrations that peaked at ~9 au (Figure 1C) when measured from the center of the chamber at approximately the animal's nose height (~2.5 cm). A comparable stimulus calibration procedure was used prior to imaging experiments to ensure that stimuli were matched across behavioral and imaging phases of the experiment.

During behavioral tests, subjects were pseudo-randomly presented with 3 trials of each of 4 odors (example protocol in Figure 1D), allowing no more than 2 consecutive trials of a given odor. These stimuli included the CS and 3 other unexposed odors that varied in chemical similarity to the CS, including a similar ester (ethyl valerate, EV, smells very similar to MV), a less-similar ester (*n*-butyl acetate, BA, which is readily discriminable from MV), and a ketone (2-hexanone, 2H, smells very different from MV). Sessions were recorded, tracked, and analyzed with FreezeFrame4 software. Individual freezing thresholds were determined off-line from each subject's motion index histogram, and an animal was considered to be freezing if its motion index was below threshold for a bout that was ≥ 1 sec in duration. The average freezing threshold across all subjects in the paired group was 4.6±0.2 (min = 3.2; max = 6.7) during the 3-day test and 4.9±0.2 (min = 2.7; max = 6.7) during the 1-month retest. Freezing was scored during 3 consecutive 20-sec bins for each trial (pre-odor, odor, and post-odor). Data were analyzed with mixed-model ANOVAs and planned *post-hoc* ANOVAs that included group, odor, trial number, and trial phase as factors. Tests with multiple comparisons were Bonferroni-corrected.

We ran a series of "behavior only" experiments in parallel with the above experiment to determine: 1) if the anesthesia and imaging procedures affected olfactory fear conditioning (Supplementary Figure S1); 2) if conditional freezing is exhibited within 24 hours of training (Supplementary Figure S2); and 3) to confirm that fear generalization persists up to

1 month after learning, as well as to parse apart any behavioral extinction effects that might be induced by the 3-day test from any potential forgetting (Supplementary Figure S3).

2.3. In Vivo Optical Neurophysiology

In vivo optical imaging was performed (Czarnecki, Moberly, Rubinstein, Turkel, Pottackal, & McGann, 2011; Czarnecki, Moberly, Turkel, Rubinstein, Pottackal, Rosenthal et al., 2012; Fast & McGann, 2017; Kass, Czarnecki, Moberly, & McGann, 2017; Kass, Guang, Moberly, & McGann, 2016; Kass, Moberly, & McGann, 2013a; Kass, Moberly, Rosenthal, Guang, & McGann, 2013b; Kass, Pottackal, Turkel, & McGann, 2013c; Kass et al., 2013d) to visualize odor-evoked GCaMP signals from GAD65-expressing PG interneurons (Figure 1G–I) before and after conditioning (Figure 1A). Vapor dilution olfactometry was used during imaging (Czarnecki et al., 2011; Czarnecki et al., 2012; Kass et al., 2017; Kass et al., 2016; Kass et al., 2013a; Kass et al., 2013b; Kass et al., 2013c; Kass et al., 2013d) to present up to 3 concentrations of up to 5 monomolecular odorants that have no known innate valence. The odor-panel was selected based on previous experiments (Kass et al., 2013b; Kass et al., 2013d), and included 3 esters (MV, which was used as the CS, EV, and BA), 1 ketone (2H), and 1 aldehyde (t*rans*-2-methyl-2-butenal, 2M2B), yielding 3 odor categories for paired and odor-alone subjects (training ester, unexposed esters, and unexposed “other”) and 1 odor category for shock-alone subjects (unexposed odors). Blocks of 3–6 trials (20-sec/trial, 60-sec ITI) were presented to anesthetized subjects. Respiration was monitored (Kass et al., 2017; Kass et al., 2013d), and odor presentations (6-sec/presentation) were timed to begin during the exhalation phase of the respiration cycle to ensure reliable odor concentrations during the first inhalation of odor.

Optical signals were analyzed as previously reported (Czarnecki et al., 2011; Czarnecki et al., 2012; Fast & McGann, 2017; Kass et al., 2017; Kass et al., 2016; Kass et al., 2013a; Kass et al., 2013b; Kass et al., 2013c; Kass et al., 2013d). Odor-evoked response amplitudes (ΔF/Fs) were quantified as the change in fluorescence during the first inhalation of odor and as the integrated change from baseline fluorescence during the 6-sec odor presentation. Glomerular regions of interest (ROIs) were matched across imaging sessions for each subject. The raw data set included 787 glomerular ROIs from 8 paired subjects, 443 ROIs from 5 shock-alone subjects, and 464 ROIs from 5 odor-alone subjects. Candidate ROIs were included as responses if the mean odor-evoked GCaMP signal across 3–6 trials was greater than 3 standard errors above 0.

ΔF/Fs were normalized relative to the maximum ΔF/F within each odor and across all imaging sessions per subject (Figures 1–2), and the corresponding number of odor-evoked glomerular responses was quantified (Figure 3). Odor-response selectivity (Figure 4) was quantified as the number of odors (from 0–5) that evoked a response in each glomerulus and similarity indexes (Soucy, Albeanu, Fantana, Murthy, & Meister, 2009) were calculated across pairs of PG cell activity maps. Correlational analyses (Figure 5) related the magnitude of baseline ΔF/Fs and change indexes computed as $(Post_{\Delta F/F}\text{-}Pre_{\Delta F/F})/(Post_{\Delta F/F}+Pre_{\Delta F/F})$. For sensitivity analyses (Figure 6), ΔF/Fs were normalized across concentrations and imaging sessions.

Statistical analyses included omnibus factorials to assess planned interactions across groups, imaging sessions, odors, and concentrations. These were followed with planned *post-hoc* ANOVAs and *t*-tests. Differences across glomerular distributions were assessed with Wilcoxon signed-ranks tests, Friedman's ANOVAs, and Kruskal-Wallis tests. *P* values were adjusted for multiple comparisons.

3. Results

3.1. Long-Lasting Generalization of Conditioned Fear to Odors

To induce generalized fear of odors, we employed a conditioning paradigm (Figure 1A–C) in which 1 day of non-discriminative training (Aizenberg & Geffen, 2013; Chen et al., 2011; Resnik & Paz, 2015) included 10 paired presentations of a single odor with a strong footshock (Baldi et al., 2004; Fanselow, 1980; Ghosh & Chattarji, 2015; Laxmi et al., 2003; Poulos et al., 2016; Shaban et al., 2006). This model parallels naturally occurring traumatic events, which are very salient and do not alternate between threatening and safe stimuli (Resnik & Paz, 2015).

During testing 3 days post-conditioning (Figure 1A, 3-day test), there was a significant difference in odor-evoked freezing between groups (Figure 1E, left, main effect of group from group×odor×trial ANOVA, $F_{(2,25)} = 232.461$, $p < 0.001$, $\eta_p^2 = 0.949$). Regardless of which odor was being presented (non-significant group×odor interaction, $F_{(6,75)} = 0.604$, $p = 0.727$, $\eta_p^2 = 0.046$), paired mice exhibited significantly (Ps < 0.001 by Bonferroni-corrected group comparisons) more odor-evoked freezing than shock-alone and odor-alone controls (which did not differ from each other, $p = 0.189$). Remarkably, paired subjects froze equally to all 4 odors (Figure 1E, left, non-significant effect of odor from *post-hoc* odor×trial ANOVA in paired group, $F_{(3,36)} = 0.666$, $p = 0.578$, $\eta_p^2 = 0.053$), demonstrating broad fear generalization. Importantly, they did not freeze continuously (Figure 1D,F and Supplementary Figure S1E), exhibiting comparable freezing to shock-alone controls prior to odor onset, and then freezing much more during the odor and immediate post-odor periods (Figure 1F, left, interaction between trial phase and group, $F_{(4,50)} = 61.472$, $p < 0.001$, $\eta_p^2 = 0.831$). These mice were tested 3 days post-training to permit interleaved imaging sessions (Figure 1A), but parallel experiments demonstrated that the imaging procedures did not influence fear generalization (Supplementary Figure S1), and that fear generalization is observed as early as 24 hours post-conditioning (Supplementary Figure S2).

To determine if the observed fear generalization parallels the long-lasting phenotype that occurs in anxiety (Jovanovic & Ressler, 2010), we performed a second behavioral test 1 month post-training (Figure 1A) and analyzed the resulting data with a 3-way ANOVA that included group, odor, and trial number as factors. The behavioral effects olfactory fear conditioning were relatively persistent because during the 1-month retest paired mice continued to exhibit generalized freezing behavior to all 4 odors (Figure 1E, right), while shock-alone and odor-alone controls continued to show minimal odor-evoked freezing (significant main effect between groups, $F_{(2,25)} = 43.225$, $p < 0.001$, $\eta_p^2 = 0.776$; non-significant group×odor interaction, $F_{(6,75)} = 1.234$, $p = 0.299$, $\eta_p^2 = 0.090$). However, when we extended these analyses by adding test session as factor to compare odor-evoked freezing between the 3-day test and the 1-month retest we identified an interaction between training

group and test session (Figure 1E, $F_{(2,25)} = 9.332$, $p = 0.001$, $\eta_p^2 = 0.427$). *Post-hoc* analyses demonstrated that paired mice exhibited a reduction in odor-evoked freezing during the 1-month retest compared to the 3-day test (Figure 1E–F, main effect of test session, $F_{(1,12)} = 19.719$, $p = 0.001$, $\eta_p^2 = 0.622$), regardless of which odor was being presented (non-significant test×odor interaction, $F_{(3,36)} = 1.244$, $p = 0.308$, $\eta_p^2 = 0.094$; non-significant effect of odor across both tests, $F_{(3,36)} = 2.089$, $p = 0.119$, $\eta_p^2 = 0.148$). This reduction likely reflects partial extinction learning during the 3-day test rather than forgetting during the month-long delay between tests, because a parallel experiment found no difference in freezing between mice tested for the first time 3 days post-training and those tested for the first time 1 month post-training (Supplementary Figure S3). By contrast, shock-alone (non-significant effect of test session from *post-hoc* ANOVA, $F_{(1,7)} = 0.063$, $p = 0.809$, $\eta_p^2 = 0.009$) and odor-alone (non-significant effect of test session from *post-hoc* ANOVA, $F_{(1,6)} = 0.259$, $p = 0.629$, $\eta_p^2 = 0.041$) controls exhibited no change in odor-evoked freezing between tests (Figure 1E,F).

3.2. Long-Lasting Enhancement of CS-Evoked PG Interneuron Activity after Conditioning

We used reporter mice (Chen et al., 2013; Taniguchi et al., 2011; Zariwala et al., 2012) to visualize CS-evoked GCaMP signals in populations of PG interneurons (Fast & McGann, 2017; Wachowiak et al., 2013) 1 day before, 1 day after, and 1 month after fear conditioning (Figure 1A). Because of the orderly mapping of odor receptors in the nose onto the olfactory bulb glomeruli, odors evoke focal increases in fluorescence in PG cells innervating odor-specific subsets of glomeruli (Figure 1G–I). These odor-evoked response maps were compared across imaging sessions between groups of animals and populations of glomeruli.

There was a significant interaction between group and imaging session on PG cell activity that was evoked by the first inhalation of the CS (Figure 1J–L and Figure 1M, left, $F_{(4,30)} = 8.279$, $p < 0.001$, $\eta_p^2 = 0.525$). Follow-up analyses demonstrated that paired mice (see Supplementary Figure S4 and Supplementary Table S1 for individual variability) exhibited a strong facilitation of CS-evoked activity after fear conditioning (Figure 1M, left, main effect of imaging session from *post-hoc* ANOVA on paired data, $F_{2,14} = 11.219$, $p = 0.001$, $\eta_p^2 = 0.616$; Figure 1N, Friedman's ANOVA, $\chi 2_{(df=2)} = 105.771$, $p < 0.001$). Specifically, there was a robust enhancement of CS-evoked GCaMP signals 1 day after conditioning (Figure 1N, *post-hoc* pre versus 1d post, $p < 0.001$) that persisted up to 1 month later (Figure 1N, *post-hoc* pre versus 1m post, $p = 0.004$), albeit to a lesser extent that the initial enhancement (Figure 1N, *post-hoc* 1d post versus 1m post, $p < 0.001$). This sensory facilitation may not require feedback from other brain regions because it was even visible during the rising phase of the first inhalation (Figure 1J). Identical results were obtained when GCaMP signals were integrated across the entire 6-sec CS presentation (Figure 1M, right and Supplementary Figure S5A,D,G), with all individual subjects exhibiting significant enhancements (Supplementary Figure S6 and Supplementary Table S2)

The odor-alone control group showed no change across imaging sessions in MV-evoked activity on the first inhalation (Figure 1I,L,M, non-significant effect of imaging session from *post-hoc* ANOVA, $F_{(2,8)} = 2.356$, $p = 0.157$, $\eta_p^2 = 0.371$) or integrated across the odor presentation (Figure 1M, right, non-significant effect of imaging session from *post-hoc*

ANOVA, $F_{(2,8)} = 0.120$, $p = 0.888$, $\eta_p^2 = 0.371$; Supplementary Figure S5C,F,G). Unexpectedly, PG cell physiology was altered in shock-alone controls that received multiple footshocks but no odors during training (Figure 1H,K,M,O). After training, shock-alone subjects tended to exhibit a small, but persistent reduction of MV-evoked GCaMP signals during the first inhalation (Figure 1M, left, effect of imaging session from *post-hoc* ANOVA, $F_{(2,8)} = 5.283$, $p = 0.034$, $\eta_p^2 = 0.569$; and Figure 1O, Friedman's ANOVA, $\chi 2_{(df=2)} = 84.351$, $p < 0.001$) and also integrated across multiple inhalations (Figure 1M, right and Supplementary Figure S5B,E,G). The opposing effects that occurred in the paired and shock-alone groups, but not in the odor-alone group, could not be attributed to differences in respiration between groups (Figure 1P, non-significant effect of group, $F_{(2,15)} = 1.129$, $p = 0.349$, $\eta_p^2 = 0.131$) or across imaging sessions (non-significant group×session interaction, $F_{(4,30)} = 1.560$ $p = 0.211$).

3.3. Neural Generalization to Non-Threatening Odors and Correlation with Freezing Behavior

We also visualized neural responses to unexposed odors before and after conditioning (Figure 2A–C). After conditioning with MV as the CS, all paired subjects (Supplementary Figure S7 and Supplementary Table S3) exhibited an enhancement of the PG cell activity that was evoked by all of the unexposed odors (Figure 2A,D,G, main effect of imaging session in paired group, $F_{(2,14)} = 8.989$, $p = 0.003$, $\eta_p^2 = 0.532$). This enhancement was comparable across odors (Figure 2A, non-significant interaction between unexposed odors and imaging session, $F_{(2,14)} = 0.320$, $p = 0.731$, $\eta_p^2 = 0.044$; Supplementary Figure S8), and equivalent in magnitude to the change in CS-evoked activity (Figures 1J,M vs. 2D,G, non-significant odor-category×prep interaction, $F_{(4,28)} = 0.156$, $p = 0.958$, $\eta_p^2 = 0.022$), paralleling the observed behavioral generalization (Figure 1E). This generalized sensory facilitation after fear conditioning cannot be attributed to respiratory effects (Supplementary Figure S8G). No changes were observed in the odor-alone control group (Figure 2C,F,G), while the shock-alone control group exhibited a modest reduction in their responses to these odors (Figure 2B,E,G).

The tested odors activate distinct but overlapping sets of glomeruli because they have some chemical similarities. Consequently, there was some overlap between the population of glomeruli that responded to the CS and the populations that responded to the unexposed odors. If fear conditioning had only enhanced activity in glomeruli driven by the CS, then the degree of generalization would depend on the degree of overlap between each odor and the CS, as occurs in generalization gradients (Aizenberg & Geffen, 2013; Lissek et al., 2008; Resnik et al., 2011). However, that is not what we observed – instead, all odors were equally facilitated and equally fearful. This suggested that olfactory fear conditioning had actually induced plasticity in glomeruli that did not respond to the CS at all. To test this, we isolated a subset of glomeruli that were activated by unexposed odors but did not respond to the CS at baseline (e.g., Figure 2H), and compared their response to their preferred odors before and after conditioning. Surprisingly, responses in these glomeruli were facilitated (Figure 2I, effect of imaging session via Friedman's ANOVA, $\chi 2_{(df=2)} = 120.096$) 1 day (*post-hoc* comparison to pre, $p < 0.001$) and 1 month (*post-hoc* comparison to pre, $p < 0.001$) after fear conditioning (though the enhancement was slightly less robust 1 month post-training, *post-*

hoc comparison between 1d post and 1m post, $p < 0.001$). This facilitation did not differ among unexposed odors (Supplementary Figure S9).

There was some variability across animals in both physiological (Supplementary Figures S4 and S6-S7) and behavioral responses to odors after conditioning. Remarkably, there was a significant positive correlation such that the subjects exhibiting the largest proportional enhancements of odor-evoked PG cell activity across all odors 1 day after training also tended to spend the most time freezing to odors during the 3-day test (Figure 2J, $r = 0.728$, $p = 0.040$).

3.4. Broader Odor Tuning and Increased Similarity of Odor Representations after Fear Generalization

There was an interaction between training group and imaging session in the number of odor-evoked glomerular responses (Figure 3, $F_{(4,30)} = 6.352$, $p = 001$, $\eta_p^2 = 0.459$). Specifically, paired conditioning modestly increased the number of glomeruli exhibiting a measureable response to each odor in the panel across imaging sessions (Figure 3A,D, main effect of imaging session from *post-hoc* ANOVA, corrected for lack of sphericity, $F_{(1.2,8.1)} = 9.796$, $p = 0.002$, $\eta_p^2 = 0.583$), whereas no difference was observed after shock-alone (Figure 3B,E, non-significant effect of imaging session from *post-hoc* ANOVA, $F_{(2,8)} = 1.053$, $p = 0.393$, $\eta_p^2 = 0.208$) or odor-alone (Figure 3C,F, non-significant effect of imaging session from *post-hoc* ANOVA, $F_{(2,8)} = 1.557$, $p = 0.269$, $\eta_p^2 = 0.280$) training. This change reflected a decrease in the odor-selectivity of individual glomeruli after paired training, but not after shock-alone or odor-alone training (Figure 4A–J, as indicated by the group×session interaction, $F_{(4,30)} = 8.110$, $p < 0.001$, $\eta_p^2 = 0.520$). On average, individual glomeruli (e.g., Figure 4G) responded to slightly more odors after paired conditioning (main effect of imaging session in paired group, $F_{(2,14)} = 16.781$, $p < 0.001$, $\eta_p^2 = 0.706$; pre, 1.64±0.04; 1d-post, 2.02±0.04; 1m-post, 1.87±0.04). This tuning shift included glomeruli that did not respond to any odors at baseline but began responding to 1 or more odors after conditioning (Supplementary Figure S9A,C,G).

The relative decrease in odor selectivity could potentially contribute to the generalized behavioral fear by increasing the similarity between neural representations of different odors. To quantify this, we calculated similarity indexes (ranging from 0–1) between pairs of PG cell activity maps (e.g., CS-EV, CS-BA, etc.) before and after conditioning. Pre-training neural representations reflected the chemical and perceptual similarity between odors (Figure 4K, pre). After conditioning, the representations of unexposed odors tended to become more similar to that of the CS (Figure 4K,L) and to each other (Supplementary Figure S10). The largest proportional changes occurred in pairs that were relatively dissimilar at baseline (e.g., Figure 4K,L, CS versus 2M2B). However, even after this change, most similarity indexes were still well below 1 (Figure 4K), suggesting that neural representations of non-threatening odors remained discriminable from the CS.

3.5. Fear Conditioning Preferentially Boosts CS-Evoked Activity in Weakly-Responsive Glomeruli

On average, CS-evoked activity was robustly increased in paired subjects, and slightly reduced in shock-alone subjects (Figure 1M). However, there is broad variance in response to the CS across glomeruli at baseline (Figure 5A–F). To test whether fear conditioning had equivalent effects on glomeruli that were weakly- and strongly-responsive at baseline, we compared baseline responsiveness to the effect of fear conditioning in individual glomeruli. Glomeruli that were most weakly activated by the CS at baseline tended to exhibit the largest enhancement of CS-evoked PG cell activity 1 day (Figure 5G, $r = -0.627$, $p < 0.001$) and 1 month ($r = -0.618$, $p < 0.001$) after paired training. By contrast, the day after shock-alone exposure, MV-evoked responses tended to be reduced in glomeruli that exhibited the largest amplitudes at baseline (Figure 5H, $r = -0.157$, $p = 0.009$).

To more clearly illustrate these relationships, glomeruli were ranked from lowest-to-highest based on pre-training MV-evoked ΔF/Fs within each group, and then separated into quartiles of the pre-training distributions (Figure 5I). After conditioning, the glomeruli in the bottom 75% of the paired distribution (Figure 5I, left) were enhanced relative to baseline (Ps < 0.001 by 1-sample t tests), whereas glomeruli within the top 25% of the pre-training response distribution were unchanged ($p = 0.920$). By contrast, glomeruli in the bottom half of the shock-alone distribution exhibited no change in response amplitude 1 day post-training (Figure 5I, right, Ps > 0.05 by 1-sample t tests), while those in the top half of the distribution were reduced relative to baseline (Figure 5I, right, Ps < 0.001 by 1-sample t tests).

3.6. Olfactory Fear Conditioning Increases Odor Sensitivity in PG Interneurons

Higher odor concentrations evoke stronger activity in the olfactory bulb (Meister & Bonhoeffer, 2001; Stewart, Kauer, & Shepherd, 1979), so the preferential boosting of weak activity could increase the sensitivity of the system to lower concentrations. To test this, we compared PG cell activity across a 4-fold range of odor concentrations. Before conditioning, the lowest concentration evoked the weakest responses and the highest concentration evoked the strongest responses (Figure 6A–I, pre), as expected. After fear generalization, paired subjects exhibited enhanced responses across all tested concentrations of the CS (Figure 6A,D,G, main effect of imaging session across concentrations, $F_{(2,14)} = 12.525$, $p = 0.001$, $\eta_p^2 = 0.641$) and the unexposed odors (Supplementary Figure S11). The proportional effect of fear conditioning was inversely related to the effect of concentration at baseline (Figure 6J) because lower concentrations evoked weaker baseline responses that were preferentially boosted, as in Figure 5. Note that after conditioning the response to the lowest concentration of the CS was even larger than the activity evoked by the highest CS concentration at baseline (Figure 6G), demonstrating that the effect of fear conditioning on PG cell activity was even greater than the effect of quadrupling the odor concentration.

Odor-alone training had no effect on sensitivity to the exposed odor (Figure 6C,F,I, non-significant effect of imaging session across concentrations, $F_{(2,8)} = 1.855$, $p = 0.218$, $\eta_p^2 = 0.317$) or to unexposed odors (Supplementary Figure S11). However, shock-alone training induced a modest but persistent decrease in PG cell activity across a range of concentrations

of MV (Figure 6B,E,H, marginally-significant effect across sessions, $F_{(2,8)} = 4.423$, $p = 0.051$, $\eta_p^2 = 0.525$), suggesting that footshock exposure by itself may cause slight decreases in sensitivity to odors (see Supplementary Figure S11 for other unexposed odors).

4. Discussion

Here, we used fear conditioning to explore the neurosensory effects of generalized fear across odors. Conditioning resulted in equivalent fear of multiple odors, regardless of similarity to the CS. This fear was correlated with large changes in early sensory processing, including hyper-responsiveness of PG cells, broadened odor tuning, and increased neural sensitivity to lower odor concentrations. These generalized effects occurred within 24 hours of conditioning, persisted for at least a month (with some evidence of reversal with extinction), and were detectable even in the first moments of the brain's response to odors. The finding that fear generalization alters early neural processing of harmless sensory cues may have important implications for the etiology and treatment of anxiety disorders.

Anxiety disorders, especially PTSD, include sensory symptoms like hypervigilance and attentional bias (Bar-Haim, Lamy, Pergamin, Bakermans-Kranenburg, & van, 2007; Dowd, Mitroff, & LaBar, 2016; Eldar, Yankelevitch, Lamy, & Bar-Haim, 2010; Krusemark & Li, 2012; McNally, Kaspi, Riemann, & Zeitlin, 1990; Notebaert, Crombez, Van Damme, De Houwer, & Theeuwes, 2011). Recent evidence suggests these symptoms may be caused by hyper-reactivity in sensory processing circuitry (Bryant et al., 2005; Clark, Galletly, Ash, Moores, Penrose, & McFarlane, 2009; Krusemark & Li, 2012; Mueller-Pfeiffer et al., 2013; Stewart & White, 2008), such as in visual cortex while viewing trauma-associated cues (Todd et al., 2015), or even at rest as part of a hypervigilant sensory state (Clancy et al., 2017). However, the alterations in sensory processing observed in PTSD reflect a balance of content specificity and generalization to trauma-related stimuli (Cortese, Leslie, & Uhde, 2015; Todd et al., 2015; Zinchenko, Al-Amin, Alam, Mahmud, Kabir, Reza et al., 2017). For instance, PTSD-suffering survivors of a building collapse show attentional bias to pictures of buildings and not faces, but this bias includes buildings other than the one that collapsed (Zinchenko et al., 2017). In humans, fear generalization thus seems to be based more on shared stimulus categories than on shared features (Dunsmoor & Murphy, 2015; Dunsmoor et al., 2011b), such that conceptual inference may allow the transfer of learned fear to harmless stimuli that vary quite considerably from a threat-predictive stimulus (Dunsmoor & Murphy, 2015). Indeed, recent studies have found that humans will generalize conditioned fear across superordinate object categories that contain vastly different category members (for example animals ranging from a dog to an elephant to a frog or tools ranging from a screwdriver, to a saw, to a measuring tape) (Dunsmoor, Kragel, Martin, & LaBar, 2014; Dunsmoor, Martin, & LaBar, 2012). Though it is challenging to assess this kind of conceptual generalization in laboratory animals, our study loosely supports a category-based learning model because mice exhibited generalized fear to "odors" rather than to "methyl valerate-like odors." We did not assess the full categorical scope of this generalization, for instance by assessing defensive behavior in response to stimuli from other sensory modalities, so we cannot rule out the possibility that mice were generalizing conditioned fear to a superordinate category that includes all novel stimuli. Nonetheless, these data demonstrate that when fear generalizes across quite different odors that the brain's earliest

olfactory sensory regions show strongly facilitated responses that do not require overlapping chemical features between the CS and other stimuli, as we observed clear evidence of facilitated responding in glomeruli that did not respond to the CS. Because odors have been hypothesized to contribute to the pathophysiology of PTSD (Cortese et al., 2015), and because the sensory capabilities of the human olfactory system are generally similar to that of other mammalian species (McGann, 2017), these findings may offer insight into the neurophysiological factors that contribute to pathological fear.

We observed that broad fear generalization was accompanied by modest changes in the odor tuning of olfactory bulb glomeruli, causing non-threatening odor representations to become more similar to each other and to the representation of the shock-predictive odor. This contrasts with discriminative conditioning, which increases the difference between the representations of threat-predictive and explicitly safe odors (Kass et al., 2013d; Li et al., 2008), and pseudo-conditioning with unpaired odor and shock presentations, which does not affect odor selectivity of cortical neurons (Chen et al., 2011). Such plasticity could potentially underlie the perceptual effects of fear conditioning, including either increases or decreases in odor discrimination acuity (Ahs et al., 2013; Chen et al., 2011; Fletcher & Wilson, 2002; Li et al., 2008) depending on the training parameters (Aizenberg & Geffen, 2013; Baldi et al., 2004; Chapuis & Wilson, 2012; Chen et al., 2011; Fanselow, 1980; Ghosh & Chattarji, 2015; Laxmi et al., 2003; Poulos et al., 2016; Shaban et al., 2006). However, even with the increase in similarity between odor representations that occurred after fear generalization, the neural representations of different odors were still quite dissimilar (Figure 4K). This suggests that mice are not behaviorally generalizing because they are mistaking other odors for the CS, but they are now representing all odors as potential threats. Notably, PG interneuron activity exhibited enhanced sensitivity to the shock-predictive odor as well as to non-threatening odors, suggesting that the behavioral generalization may have been mediated by a global facilitation of threat detection (Resnik et al., 2011) across a dangerous category of sensory stimuli. Thus, the increased odor-evoked neural activity likely serves non-perceptual functions, such as providing a “warning signal” to recruit attention or prioritize the odor for evoking defensive behavior.

The mechanism of the observed plasticity presumably involves the amygdala, which is a key structure in fear learning (LeDoux, 2000; Maren & Quirk, 2004; Phelps & LeDoux, 2005) that has been implicated in anxiety disorders such as PTSD (Bryant et al., 2005; Jovanovic & Ressler, 2010; Liberzon, Taylor, Amdur, Jung, Chamberlain, Minoshima et al., 1999; Protopopescu, Pan, Tuescher, Cloitre, Goldstein, Engelien et al., 2005; Rauch, Whalen, Shin, McInerney, Macklin, Lasko et al., 2000; Stevens, Kim, Galatzer-Levy, Reddy, Ely, Nemeroff et al., 2017), and also LC noradrenaline, which is involved in odor perception, olfactory learning, and odor memory formation (Eckmeier & Shea, 2014; Linster, Nai, & Ennis, 2011; Mandairon, Peace, Karnow, Kim, Ennis, & Linster, 2008; Moreno, Bath, Kuczewski, Sacquet, Didier, & Mandairon, 2012; Sullivan, Stackenwalt, Nasr, Lemon, & Wilson, 2000; Sullivan, Zyzak, Skierkowski, & Wilson, 1992). Recent studies using auditory fear conditioning have found that the specificity of cue-evoked freezing is paralleled by the specificity of cue-evoked amygdala activity (Ghosh & Chattarji, 2015), and that the effect of fear generalization on tuning curves in the amygdala was dependent upon the neuron’s preferred stimulus, with the broadest shifts in tuning occurring when the preferred stimulus

was relatively far from the CS (Resnik & Paz, 2015). Comparable effects of fear generalization are reported here, with glomeruli that exhibited the weakest responses before conditioning being robustly facilitated and the largest baseline responses showing minimal change. We recently demonstrated that PG interneuron activity is influenced by the output of the amygdala and that this effect is mediated by interactions with LC (Fast & McGann, 2017). Notably, the amygdala-dependent noradrenergic tuning of PG circuitry preferentially affected weakly- over strongly-activated glomeruli, paralleling the effect of fear generalization.

Unexpectedly, odor-evoked PG interneuron activity was reduced in the shock-alone group, even though these subjects did not experience discrete odor cues during conditioning. However, LC densely innervates the olfactory bulb (Linster et al., 2011; Shipley & Ennis, 1996) and salient events can stimulate LC noradrenaline release (Aston-Jones et al., 1996). Further, LC stimulation that is delivered in the absence of any odors induces a subsequent suppression of odor-evoked responses in the olfactory bulb (Eckmeier & Shea, 2014), consistent with the decrease in sensitivity that was observed here. It is possible that the highly aversive (and salient) footshocks stimulated noradrenaline release in the olfactory bulb, resulting in plasticity in PG interneurons.

In sum, these data show that broad fear generalization is associated with enhanced processing of threat-related stimuli, and that this sensory plasticity is relatively long-lasting, paralleling the pathological fear that can persist for years after a traumatic event in humans. Activity in this circuitry might normally facilitate the detection of threating sensory cues, but perturbations in this activity might promote vigilance towards harmless cues that resemble danger cues, and thus contribute to anxiety.

Supplementary Material

Refer to Web version on PubMed Central for supplementary material.

Acknowledgments

This work was supported by the National Institute on Deafness and Other Communication Disorders [R01 DC013090 to JPM and F31 DC013719 to MDK] and the National Institute of Mental Health [R01 MH101293 to JPM)] at the National Institutes of Health. We thank Tracey Shors, Timothy Otto, Donald Wilson, and Michelle Rosenthal for helpful discussion on the project.

References

Ahs F, Miller SS, Gordon AR, Lundstrom JN. Aversive learning increases sensory detection sensitivity. Biol Psychol. 2013; 92:135–141. [PubMed: 23174695]

Aizenberg M, Geffen MN. Bidirectional effects of aversive learning on perceptual acuity are mediated by the sensory cortex. Nat Neurosci. 2013; 16:994–996. [PubMed: 23817548]

Aston-Jones G, Rajkowski J, Kubiak P, Valentino RJ, Shipley MT. Role of the locus coeruleus in emotional activation. Prog Brain Res. 1996; 107:379–402. [PubMed: 8782532]

Aungst JL, Heyward PM, Puche AC, Karnup SV, Hayar A, Szabo G, Shipley MT. Centre-surround inhibition among olfactory bulb glomeruli. Nature. 2003; 426:623–629. [PubMed: 14668854]

Bakin JS, Weinberger NM. Classical conditioning induces CS-specific receptive field plasticity in the auditory cortex of the guinea pig. Brain Res. 1990; 536:271–286. [PubMed: 2085753]

Baldi E, Lorenzini CA, Bucherelli C. Footshock intensity and generalization in contextual and auditory-cued fear conditioning in the rat. Neurobiol Learn Mem. 2004; 81:162–166. [PubMed: 15082017]

Bar-Haim Y, Lamy D, Pergamin L, Bakermans-Kranenburg MJ, van IMH. Threat-related attentional bias in anxious and nonanxious individuals: a meta-analytic study. Psychol Bull. 2007; 133:1–24. [PubMed: 17201568]

Boyd AM, Sturgill JF, Poo C, Isaacson JS. Cortical feedback control of olfactory bulb circuits. Neuron. 2012; 76:1161–1174. [PubMed: 23259951]

Bryant RA, Felmingham KL, Kemp AH, Barton M, Peduto AS, Rennie C, Gordon E, Williams LM. Neural networks of information processing in posttraumatic stress disorder: a functional magnetic resonance imaging study. Biol Psychiatry. 2005; 58:111–118. [PubMed: 16038681]

Carmichael ST, Clugnet MC, Price JL. Central olfactory connections in the macaque monkey. J Comp Neurol. 1994; 346:403–434. [PubMed: 7527806]

Chapuis J, Wilson DA. Bidirectional plasticity of cortical pattern recognition and behavioral sensory acuity. Nat Neurosci. 2012; 15:155–U194.

Chen CF, Barnes DC, Wilson DA. Generalized vs. stimulus-specific learned fear differentially modifies stimulus encoding in primary sensory cortex of awake rats. J Neurophysiol. 2011; 106:3136–3144. [PubMed: 21918001]

Chen TW, Wardill TJ, Sun Y, Pulver SR, Renninger SL, Baohan A, Schreiter ER, Kerr RA, Orger MB, Jayaraman V, Looger LL, Svoboda K, Kim DS. Ultrasensitive fluorescent proteins for imaging neuronal activity. Nature. 2013; 499:295–300. [PubMed: 23868258]

Ciocchi S, Herry C, Grenier F, Wolff SB, Letzkus JJ, Vlachos I, Ehrlich I, Sprengel R, Deisseroth K, Stadler MB, Muller C, Luthi A. Encoding of conditioned fear in central amygdala inhibitory circuits. Nature. 2010; 468:277–282. [PubMed: 21068837]

Clancy K, Ding M, Bernat E, Schmidt NB, Li W. Restless 'rest': intrinsic sensory hyperactivity and disinhibition in post-traumatic stress disorder. Brain. 2017; 140:2041–2050. [PubMed: 28582479]

Clark CR, Galletly CA, Ash DJ, Moores KA, Penrose RA, McFarlane AC. Evidence-based medicine evaluation of electrophysiological studies of the anxiety disorders. Clin EEG Neurosci. 2009; 40:84–112. [PubMed: 19534302]

Cortese BM, Leslie K, Uhde TW. Differential odor sensitivity in PTSD: Implications for treatment and future research. J Affect Disord. 2015; 179:23–30. [PubMed: 25845746]

Czarnecki LA, Moberly AH, Rubinstein T, Turkel DJ, Pottackal J, McGann JP. In vivo visualization of olfactory pathophysiology induced by intranasal cadmium instillation in mice. Neurotoxicology. 2011; 32:441–449. [PubMed: 21443902]

Czarnecki LA, Moberly AH, Turkel DJ, Rubinstein T, Pottackal J, Rosenthal MC, McCandlish EF, Buckley B, McGann JP. Functional rehabilitation of cadmium-induced neurotoxicity despite persistent peripheral pathophysiology in the olfactory system. Toxicol Sci. 2012; 126:534–544. [PubMed: 22287023]

de Olmos J, Hardy H, Heimer L. The afferent connections of the main and the accessory olfactory bulb formations in the rat: an experimental HRP-study. J Comp Neurol. 1978; 181:213–244. [PubMed: 690266]

Dias BG, Ressler KJ. Parental olfactory experience influences behavior and neural structure in subsequent generations. Nat Neurosci. 2014; 17:89–96. [PubMed: 24292232]

Dowd EW, Mitroff SR, LaBar KS. Fear generalization gradients in visuospatial attention. Emotion. 2016; 16:1011–1018. [PubMed: 27213724]

Dunsmoor JE, Kragel PA, Martin A, LaBar KS. Aversive learning modulates cortical representations of object categories. Cereb Cortex. 2014; 24:2859–2872. [PubMed: 23709642]

Dunsmoor JE, Martin A, LaBar KS. Role of conceptual knowledge in learning and retention of conditioned fear. Biol Psychol. 2012; 89:300–305. [PubMed: 22118937]

Dunsmoor JE, Mitroff SR, LaBar KS. Generalization of conditioned fear along a dimension of increasing fear intensity. Learn Mem. 2009; 16:460–469. [PubMed: 19553384]

Dunsmoor JE, Murphy GL. Categories, concepts, and conditioning: how humans generalize fear. Trends Cogn Sci. 2015; 19:73–77. [PubMed: 25577706]

Dunsmoor JE, Paz R. Fear Generalization and Anxiety: Behavioral and Neural Mechanisms. Biol Psychiatry. 2015; 78:336–343. [PubMed: 25981173]

Dunsmoor JE, Prince SE, Murty VP, Kragel PA, LaBar KS. Neurobehavioral mechanisms of human fear generalization. Neuroimage. 2011a; 55:1878–1888. [PubMed: 21256233]

Dunsmoor JE, White AJ, LaBar KS. Conceptual similarity promotes generalization of higher order fear learning. Learn Mem. 2011b; 18:156–160. [PubMed: 21330378]

Eckmeier D, Shea SD. Noradrenergic plasticity of olfactory sensory neuron inputs to the main olfactory bulb. J Neurosci. 2014; 34:15234–15243. [PubMed: 25392492]

Eldar S, Yankelevitch R, Lamy D, Bar-Haim Y. Enhanced neural reactivity and selective attention to threat in anxiety. Biol Psychol. 2010; 85:252–257. [PubMed: 20655976]

Fanselow MS. Conditioned and unconditional components of post-shock freezing. Pavlov J Biol Sci. 1980; 15:177–182. [PubMed: 7208128]

Fast CD, McGann JP. Amygdalar Gating of Early Sensory Processing through Interactions with Locus Coeruleus. J Neurosci. 2017; 37:3085–3101. [PubMed: 28188216]

Fletcher ML. Olfactory aversive conditioning alters olfactory bulb mitral/tufted cell glomerular odor responses. Front Syst Neurosci. 2012; 6:16. [PubMed: 22461771]

Fletcher ML, Wilson DA. Experience modifies olfactory acuity: acetylcholine-dependent learning decreases behavioral generalization between similar odorants. J Neurosci. 2002; 22:RC201. [PubMed: 11784813]

Gdalyahu A, Tring E, Polack PO, Gruver R, Golshani P, Fanselow MS, Silva AJ, Trachtenberg JT. Associative fear learning enhances sparse network coding in primary sensory cortex. Neuron. 2012; 75:121–132. [PubMed: 22794266]

Ghosh S, Chattarji S. Neuronal encoding of the switch from specific to generalized fear. Nat Neurosci. 2015; 18:112–120. [PubMed: 25436666]

Jones SV, Choi DC, Davis M, Ressler KJ. Learning-dependent structural plasticity in the adult olfactory pathway. J Neurosci. 2008; 28:13106–13111. [PubMed: 19052201]

Jovanovic T, Ressler KJ. How the neurocircuitry and genetics of fear inhibition may inform our understanding of PTSD. Am J Psychiatry. 2010; 167:648–662. [PubMed: 20231322]

Kass MD, Czarnecki LA, Moberly AH, McGann JP. Differences in peripheral sensory input to the olfactory bulb between male and female mice. Sci Rep. 2017; 7:45851. [PubMed: 28443629]

Kass MD, Guang SA, Moberly AH, McGann JP. Changes in Olfactory Sensory Neuron Physiology and Olfactory Perceptual Learning After Odorant Exposure in Adult Mice. Chem Senses. 2016; 41:123–133. [PubMed: 26514410]

Kass MD, Moberly AH, McGann JP. Spatiotemporal alterations in primary odorant representations in olfactory marker protein knockout mice. PLoS One. 2013a; 8:e61431. [PubMed: 23630588]

Kass MD, Moberly AH, Rosenthal MC, Guang SA, McGann JP. Odor-specific, olfactory marker protein-mediated sparsening of primary olfactory input to the brain after odor exposure. J Neurosci. 2013b; 33:6594–6602. [PubMed: 23575856]

Kass MD, Pottackal J, Turkel DJ, McGann JP. Changes in the neural representation of odorants after olfactory deprivation in the adult mouse olfactory bulb. Chem Senses. 2013c; 38:77–89. [PubMed: 23125347]

Kass MD, Rosenthal MC, Pottackal J, McGann JP. Fear learning enhances neural responses to threat-predictive sensory stimuli. Science. 2013d; 342:1389–1392. [PubMed: 24337299]

Krusemark EA, Li W. Enhanced Olfactory Sensory Perception of Threat in Anxiety: An Event-Related fMRI Study. Chemosens Percept. 2012; 5:37–45. [PubMed: 22866182]

Laxmi TR, Stork O, Pape HC. Generalisation of conditioned fear and its behavioural expression in mice. Behav Brain Res. 2003; 145:89–98. [PubMed: 14529808]

LeDoux JE. Emotion circuits in the brain. Annu Rev Neurosci. 2000; 23:155–184. [PubMed: 10845062]

Li W, Howard JD, Parrish TB, Gottfried JA. Aversive learning enhances perceptual and cortical discrimination of indiscriminable odor cues. Science. 2008; 319:1842–1845. [PubMed: 18369149]

Liberzon I, Taylor SF, Amdur R, Jung TD, Chamberlain KR, Minoshima S, Koeppe RA, Fig LM. Brain activation in PTSD in response to trauma-related stimuli. Biol Psychiatry. 1999; 45:817–826. [PubMed: 10202568]

Linster C, Nai Q, Ennis M. Nonlinear effects of noradrenergic modulation of olfactory bulb function in adult rodents. J Neurophysiol. 2011; 105:1432–1443. [PubMed: 21273323]

Lissek S, Biggs AL, Rabin SJ, Cornwell BR, Alvarez RP, Pine DS, Grillon C. Generalization of conditioned fear-potentiated startle in humans: experimental validation and clinical relevance. Behav Res Ther. 2008; 46:678–687. [PubMed: 18394587]

Lissek S, Kaczkurkin AN, Rabin S, Geraci M, Pine DS, Grillon C. Generalized anxiety disorder is associated with overgeneralization of classically conditioned fear. Biol Psychiatry. 2014; 75:909–915. [PubMed: 24001473]

Lissek S, Rabin S, Heller RE, Lukenbaugh D, Geraci M, Pine DS, Grillon C. Overgeneralization of conditioned fear as a pathogenic marker of panic disorder. Am J Psychiatry. 2010; 167:47–55. [PubMed: 19917595]

Liu S, Plachez C, Shao Z, Puche A, Shipley MT. Olfactory bulb short axon cell release of GABA and dopamine produces a temporally biphasic inhibition-excitation response in external tufted cells. J Neurosci. 2013; 33:2916–2926. [PubMed: 23407950]

Liu S, Shao Z, Puche A, Wachowiak M, Rothermel M, Shipley MT. Muscarinic receptors modulate dendrodendritic inhibitory synapses to sculpt glomerular output. J Neurosci. 2015; 35:5680–5692. [PubMed: 25855181]

Ma M, Luo M. Optogenetic activation of basal forebrain cholinergic neurons modulates neuronal excitability and sensory responses in the main olfactory bulb. J Neurosci. 2012; 32:10105–10116. [PubMed: 22836246]

Mandairon N, Peace S, Karnow A, Kim J, Ennis M, Linster C. Noradrenergic modulation in the olfactory bulb influences spontaneous and reward-motivated discrimination, but not the formation of habituation memory. Eur J Neurosci. 2008; 27:1210–1219. [PubMed: 18364038]

Maren S, Quirk GJ. Neuronal signalling of fear memory. Nat Rev Neurosci. 2004; 5:844–852. [PubMed: 15496862]

Markopoulos F, Rokni D, Gire DH, Murthy VN. Functional properties of cortical feedback projections to the olfactory bulb. Neuron. 2012; 76:1175–1188. [PubMed: 23259952]

McGann JP. Presynaptic inhibition of olfactory sensory neurons: new mechanisms and potential functions. Chem Senses. 2013; 38:459–474. [PubMed: 23761680]

McGann JP. Associative learning and sensory neuroplasticity: how does it happen and what is it good for? Learn Mem. 2015; 22:567–576. [PubMed: 26472647]

McGann JP. Poor human olfaction is a 19th-century myth. Science. 2017:356.

McGann JP, Pirez N, Gainey MA, Muratore C, Elias AS, Wachowiak M. Odorant representations are modulated by intra- but not interglomerular presynaptic inhibition of olfactory sensory neurons. Neuron. 2005; 48:1039–1053. [PubMed: 16364906]

McNally RJ, Kaspi SP, Riemann BC, Zeitlin SB. Selective processing of threat cues in posttraumatic stress disorder. J Abnorm Psychol. 1990; 99:398–402. [PubMed: 2266215]

Meister M, Bonhoeffer T. Tuning and topography in an odor map on the rat olfactory bulb. J Neurosci. 2001; 21:1351–1360. [PubMed: 11160406]

Miasnikov AA, Weinberger NM. Detection of an inhibitory cortical gradient underlying peak shift in learning: a neural basis for a false memory. Neurobiol Learn Mem. 2012; 98:368–379. [PubMed: 23063933]

Moreno MM, Bath K, Kuczewski N, Sacquet J, Didier A, Mandairon N. Action of the noradrenergic system on adult-born cells is required for olfactory learning in mice. J Neurosci. 2012; 32:3748–3758. [PubMed: 22423095]

Mueller-Pfeiffer C, Schick M, Schulte-Vels T, O'Gorman R, Michels L, Martin-Soelch C, Blair JR, Rufer M, Schnyder U, Zeffiro T, Hasler G. Atypical visual processing in posttraumatic stress disorder. Neuroimage Clin. 2013; 3:531–538. [PubMed: 24371791]

Murphy GJ, Darcy DP, Isaacson JS. Intraglomerular inhibition: signaling mechanisms of an olfactory microcircuit. Nat Neurosci. 2005; 8:354–364. [PubMed: 15696160]

Notebaert L, Crombez G, Van Damme S, De Houwer J, Theeuwes J. Signals of threat do not capture, but prioritize, attention: a conditioning approach. Emotion. 2011; 11:81–89. [PubMed: 21401228]

Olatunji BO, Armstrong T, McHugo M, Zald DH. Heightened attentional capture by threat in veterans with PTSD. J Abnorm Psychol. 2013; 122:397–405. [PubMed: 23148782]

Parma V, Ferraro S, Miller SS, Ahs F, Lundstrom JN. Enhancement of Odor Sensitivity Following Repeated Odor and Visual Fear Conditioning. Chem Senses. 2015; 40:497–506. [PubMed: 26126729]

Phelps EA, LeDoux JE. Contributions of the amygdala to emotion processing: from animal models to human behavior. Neuron. 2005; 48:175–187. [PubMed: 16242399]

Poulos AM, Mehta N, Lu B, Amir D, Livingston B, Santarelli A, Zhuravka I, Fanselow MS. Conditioning- and time-dependent increases in context fear and generalization. Learn Mem. 2016; 23:379–385. [PubMed: 27317198]

Protopopescu X, Pan H, Tuescher O, Cloitre M, Goldstein M, Engelien W, Epstein J, Yang Y, Gorman J, LeDoux J, Silbersweig D, Stern E. Differential time courses and specificity of amygdala activity in posttraumatic stress disorder subjects and normal control subjects. Biol Psychiatry. 2005; 57:464–473. [PubMed: 15737660]

Quirk GJ, Armony JL, LeDoux JE. Fear conditioning enhances different temporal components of tone-evoked spike trains in auditory cortex and lateral amygdala. Neuron. 1997; 19:613–624. [PubMed: 9331352]

Rajbhandari AK, Zhu R, Adling C, Fanselow MS, Waschek JA. Graded fear generalization enhances the level of cfos-positive neurons specifically in the basolateral amygdala. J Neurosci Res. 2016; 94:1393–1399. [PubMed: 27661774]

Rauch SL, Whalen PJ, Shin LM, McInerney SC, Macklin ML, Lasko NB, Orr SP, Pitman RK. Exaggerated amygdala response to masked facial stimuli in posttraumatic stress disorder: a functional MRI study. Biol Psychiatry. 2000; 47:769–776. [PubMed: 10812035]

Resnik J, Paz R. Fear generalization in the primate amygdala. Nat Neurosci. 2015; 18:188–190. [PubMed: 25531573]

Resnik J, Sobel N, Paz R. Auditory aversive learning increases discrimination thresholds. Nat Neurosci. 2011; 14:791–796. [PubMed: 21552275]

Sevelinges Y, Moriceau S, Holman P, Miner C, Muzny K, Gervais R, Mouly AM, Sullivan RM. Enduring effects of infant memories: infant odor-shock conditioning attenuates amygdala activity and adult fear conditioning. Biol Psychiatry. 2007; 62:1070–1079. [PubMed: 17826749]

Shaban H, Humeau Y, Herry C, Cassasus G, Shigemoto R, Ciocchi S, Barbieri S, van der Putten H, Kaupmann K, Bettler B, Luthi A. Generalization of amygdala LTP and conditioned fear in the absence of presynaptic inhibition. Nat Neurosci. 2006; 9:1028–1035. [PubMed: 16819521]

Shao Z, Puche AC, Kiyokage E, Szabo G, Shipley MT. Two GABAergic intraglomerular circuits differentially regulate tonic and phasic presynaptic inhibition of olfactory nerve terminals. J Neurophysiol. 2009; 101:1988–2001. [PubMed: 19225171]

Shao Z, Puche AC, Liu S, Shipley MT. Intraglomerular inhibition shapes the strength and temporal structure of glomerular output. J Neurophysiol. 2012; 108:782–793. [PubMed: 22592311]

Shipley MT, Ennis M. Functional organization of olfactory system. J Neurobiol. 1996; 30:123–176. [PubMed: 8727988]

Soucy ER, Albeanu DF, Fantana AL, Murthy VN, Meister M. Precision and diversity in an odor map on the olfactory bulb. Nat Neurosci. 2009; 12:210–220. [PubMed: 19151709]

Stevens JS, Kim YJ, Galatzer-Levy IR, Reddy R, Ely TD, Nemeroff CB, Hudak LA, Jovanovic T, Rothbaum BO, Ressler KJ. Amygdala Reactivity and Anterior Cingulate Habituation Predict Posttraumatic Stress Disorder Symptom Maintenance After Acute Civilian Trauma. Biol Psychiatry. 2017; 81:1023–1029. [PubMed: 28117048]

Stewart LP, White PM. Sensory filtering phenomenology in PTSD. Depress Anxiety. 2008; 25:38–45. [PubMed: 17203460]

Stewart WB, Kauer JS, Shepherd GM. Functional organization of rat olfactory bulb analysed by the 2-deoxyglucose method. J Comp Neurol. 1979; 185:715–734. [PubMed: 447878]

Sullivan RM, Stackenwalt G, Nasr F, Lemon C, Wilson DA. Association of an odor with activation of olfactory bulb noradrenergic beta-receptors or locus coeruleus stimulation is sufficient to produce

learned approach responses to that odor in neonatal rats. Behav Neurosci. 2000; 114:957–962. [PubMed: 11085610]

Sullivan RM, Zyzak DR, Skierkowski P, Wilson DA. The role of olfactory bulb norepinephrine in early olfactory learning. Brain Res Dev Brain Res. 1992; 70:279–282. [PubMed: 1477962]

Taniguchi H, He M, Wu P, Kim S, Paik R, Sugino K, Kvitsiani D, Fu Y, Lu J, Lin Y, Miyoshi G, Shima Y, Fishell G, Nelson SB, Huang ZJ. A resource of Cre driver lines for genetic targeting of GABAergic neurons in cerebral cortex. Neuron. 2011; 71:995–1013. [PubMed: 21943598]

Todd RM, MacDonald MJ, Sedge P, Robertson A, Jetly R, Taylor MJ, Pang EW. Soldiers With Posttraumatic Stress Disorder See a World Full of Threat: Magnetoencephalography Reveals Enhanced Tuning to Combat-Related Cues. Biol Psychiatry. 2015; 78:821–829. [PubMed: 26094019]

van Meurs B, Wiggert N, Wicker I, Lissek S. Maladaptive behavioral consequences of conditioned fear-generalization: a pronounced, yet sparsely studied, feature of anxiety pathology. Behav Res Ther. 2014; 57:29–37. [PubMed: 24768950]

Wachowiak M, Economo MN, Diaz-Quesada M, Brunert D, Wesson DW, White JA, Rothermel M. Optical dissection of odor information processing in vivo using GCaMPs expressed in specified cell types of the olfactory bulb. J Neurosci. 2013; 33:5285–5300. [PubMed: 23516293]

Weinberger NM. Associative representational plasticity in the auditory cortex: a synthesis of two disciplines. Learn Mem. 2007; 14:1–16. [PubMed: 17202426]

Zaborszky L, Carlsen J, Brashear HR, Heimer L. Cholinergic and GABAergic afferents to the olfactory bulb in the rat with special emphasis on the projection neurons in the nucleus of the horizontal limb of the diagonal band. J Comp Neurol. 1986; 243:488–509. [PubMed: 3512629]

Zariwala HA, Borghuis BG, Hoogland TM, Madisen L, Tian L, De Zeeuw CI, Zeng H, Looger LL, Svoboda K, Chen TW. A Cre-dependent GCaMP3 reporter mouse for neuronal imaging in vivo. J Neurosci. 2012; 32:3131–3141. [PubMed: 22378886]

Zinchenko A, Al-Amin MM, Alam MM, Mahmud W, Kabir N, Reza HM, Burne THJ. Content specificity of attentional bias to threat in post-traumatic stress disorder. J Anxiety Disord. 2017; 50:33–39. [PubMed: 28551393]

Highlights

- Olfactory fear learning facilitated odor-evoked periglomerular (PG) cell activity.
- Strength of learned fear correlated with degree of PG response enhancement (r=0.7).
- Generalized fear across odors paralleled generalized enhancement of PG activity.
- Plasticity occurred within 24 hours of learning and persisted for at least 1 month.
- These findings have implications for anxiety disorders with sensory sequelae.

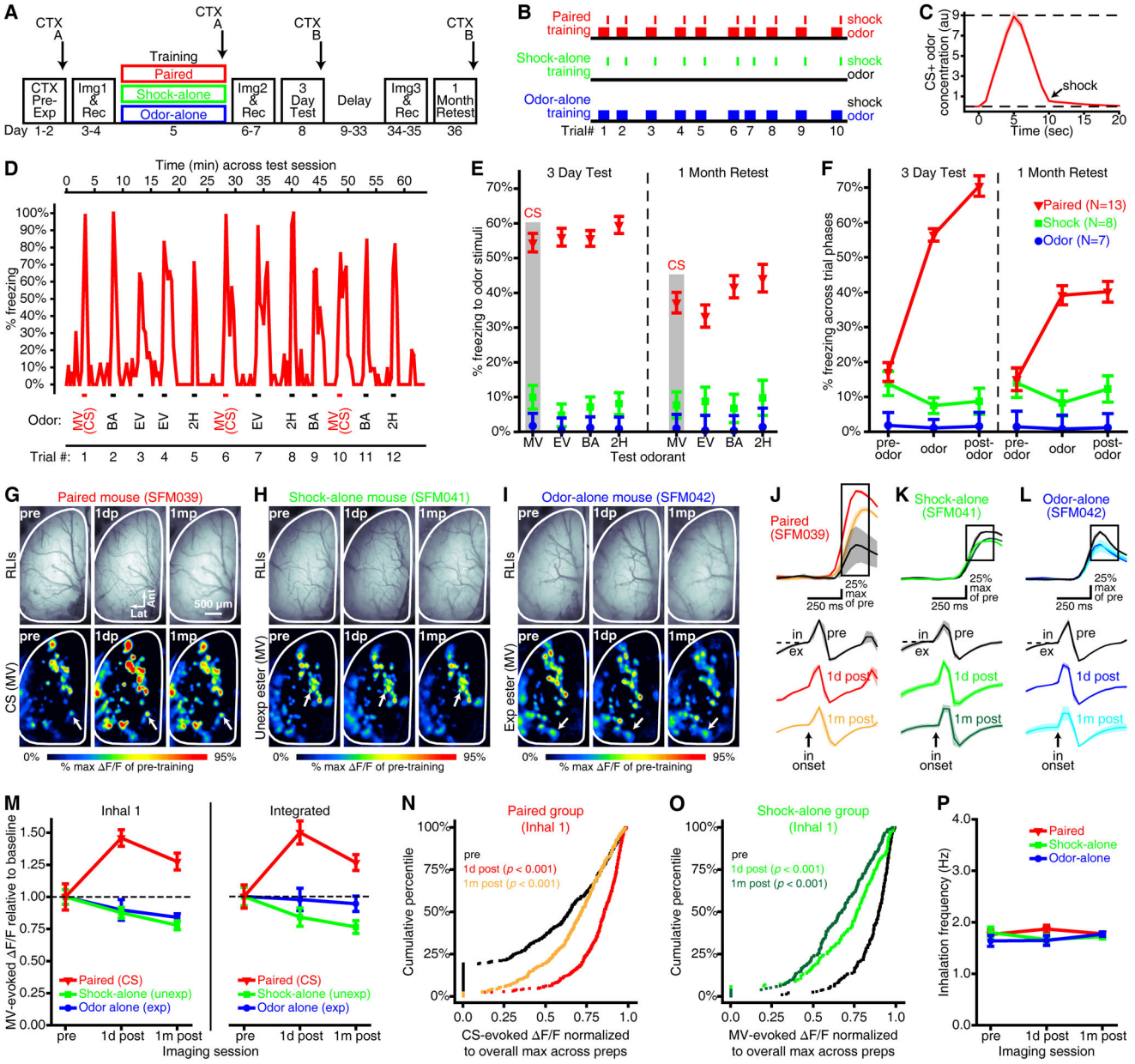

Figure 1. Olfactory fear conditioning results in a long-lasting, generalized fear response and an enhancement of CS-evoked PG interneuron activity

(A) Experimental timeline. CTX Pre-Exp, context pre-exposure; Img, imaging; Rec, recovery. **(B)** Sample paired (top), shock-alone (middle), and odor-alone (bottom) training protocols. **(C)** Mean±SEM CS concentration (in arbitrary units, au) across 10 paired trials. Dashed lines: 9 au, target concentration; 0 au, odor-free. **(D)** Representative freezing histogram that is plotted against the protocol from that paired subject's 3-day test session. Tick marks (bottom) are labeled to show odor presentations (MV/CS, EV, BA, and 2H) during all 12 trials. **(E)** Paired subjects exhibited odor-evoked freezing that generalized across odors, whereas comparatively little odor-evoked freezing was observed in either control group. These data are collapsed across odors in **F** and shown as the "odor" trial

phase. **(F)** Freezing data are pooled across all 12 trials and separated by trial phase to show relative increases and decreases in freezing that were evoked by odor presentations in the paired and shock-alone groups, respectively. **E–F** show group means±SEMs from the 3-day (left) and 1-month (right) tests. **(G–I)** Representative resting light images (RLIs) and pseudocolored difference maps from 1 day before (pre), 1 day after (1dp), and 1 month after (1mp) paired **(G)**, shock-alone **(H)**, or odor-alone **(I)** training. **(J–L)** Mean±SEM fluorescence (top; ΔF/F) and piezosensor (bottom: in, inhalation; ex, exhalation) records correspond with the glomerular callouts in **G–I**. All records are aligned relative to the first inhalation after odor onset. Boxed regions indicate the frames that were used for inhalation 1-evoked activity maps **(G–I)** and analyses **(M**, left and **N–O)**. Traces and activity maps **(G–L)** are averaged across 3–6 trials of MV, which was the CS for paired subjects, an unexposed ester for shock-alone subjects, and the exposed ester for odor-alone subjects. **(M)** Mean ±SEM CS-evoked activity during the first inhalation (left) and integrated across the entire odor presentation (right) plotted relative to baseline (dashed line) across imaging sessions. **(N–O)** Cumulative frequency histograms pooling glomeruli across subjects. CS-evoked PG cell activity was enhanced after paired training **(N)** but reduced after shock-alone training **(O)**. *P* values are compared with pre-training baseline. **(P)** Mean±SEM inhalation frequency did not differ between groups or across imaging sessions.

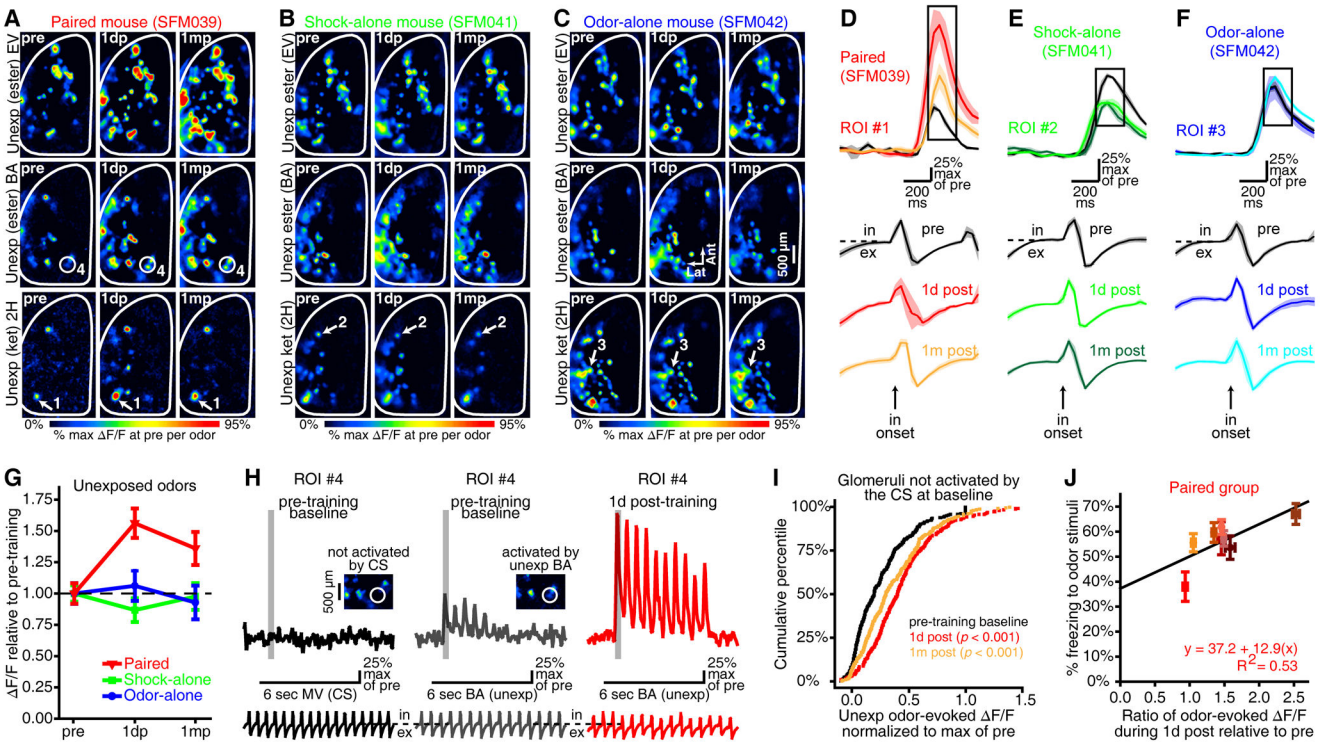

Figure 2. Generalized enhancement of odor-evoked PG interneuron activity after olfactory fear conditioning

(A–C) Activity maps from paired **(A)**, shock-alone **(B)**, and odor-alone **(C)** subjects that were evoked by 3 unexposed (unexp) odors (top, EV; middle, BA; bottom, 2H). **(D–F)** Traces show the mean±SEM odor-evoked change in fluorescence (ΔF/F, top) and respiration (bottom; in, inhalation; ex, exhalation) records 1 day before (pre), 1 day after (1d post), and 1 month after (1m post) training. Traces correspond to the numbered glomeruli in **A–C** and are aligned relative to the first inhalation after odor onset. Boxed regions note the frames that were used for inhalation 1-evoked maps **(A–C)** and analyses **(G–I)**. The examples in **A–F** are averaged across 3–6 trials. **(G)** Mean±SEM odor-evoked ΔF/F pooled across all unexposed odors for each group and plotted across imaging preparations (dashed line, pre-training baseline). **(H–I)** Glomeruli that were not activated by the CS at baseline were still facilitated after fear conditioning. **(H)** ROI #4 (which corresponds to the callout in **A**) did not respond to the CS at baseline (left), but nonetheless exhibited an enhanced response to BA after fear conditioning (middle and right). Each set of 3 traces shows ROI #4's fluorescence (top) and respiration (bottom) records relative to the 6-sec odor presentation (middle) from that trial. Inhalation 1 **(G,I)** and integrated **(J)** measurements correspond with the shaded regions and the 6-sec odor presentations, respectively. **(I)** Cumulative frequency histogram illustrating the odor-evoked ΔF/Fs in glomeruli that did not respond to the CS at baseline, but still exhibited enhanced responses to unexposed odors after fear conditioning. Data are pooled across 4 unexposed odors and 313 glomeruli that did not respond to the CS at baseline. **(J)** Odor-evoked freezing behavior (*y*-axis) was positively correlated with the relative enhancement of odor-evoked PG cell activity after fear conditioning (*x*-axis). For

each paired subject, freezing was averaged across all 12 trials during the 3-day test and odor-evoked GCaMP signals were averaged across all glomeruli and odors.

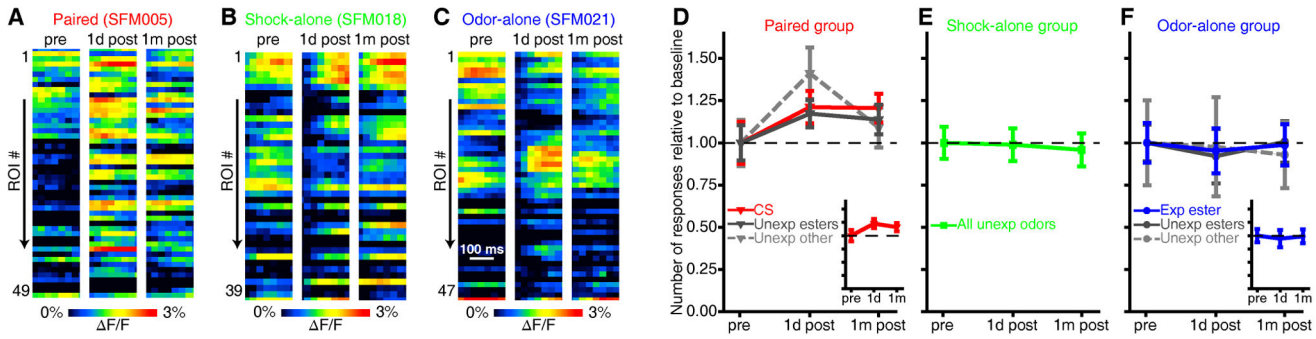

Figure 3. Olfactory fear conditioning increases the number of glomeruli exhibiting odor-evoked responses

(A–C) Pseudocolored heat maps from imaging sessions that were performed 1 day before (pre, left), 1 day after (1d post, middle), and 1 month after (1m post, right) paired **(A)**, shock-alone **(B)**, or odor-alone **(C)** training in these representative subjects. Each heat map depicts the MV-evoked change in fluorescence (ΔF/F) across a population of glomeruli (ROI #1→*N*) during a 200 ms window corresponding to the first inhalation of MV (which was, respectively, the CS and exposed ester for paired and odor-alone subjects). Examples in **A–C** are from single trials. **(D–E)** The mean±SEM number of odor-evoked glomerular responses is shown as a ratio of pre-training baseline (dashed lines centered on 1.0) and plotted as a function of imaging session for paired **(D)**, shock-alone **(E)**, and odor-alone **(F)** groups. The data are pooled across relevant odor categories for each group. The insets **(D,F)** show the mean±SEM number of responses pooled across all 3 odor categories and are scaled to the same *y*-axes of the main panels.

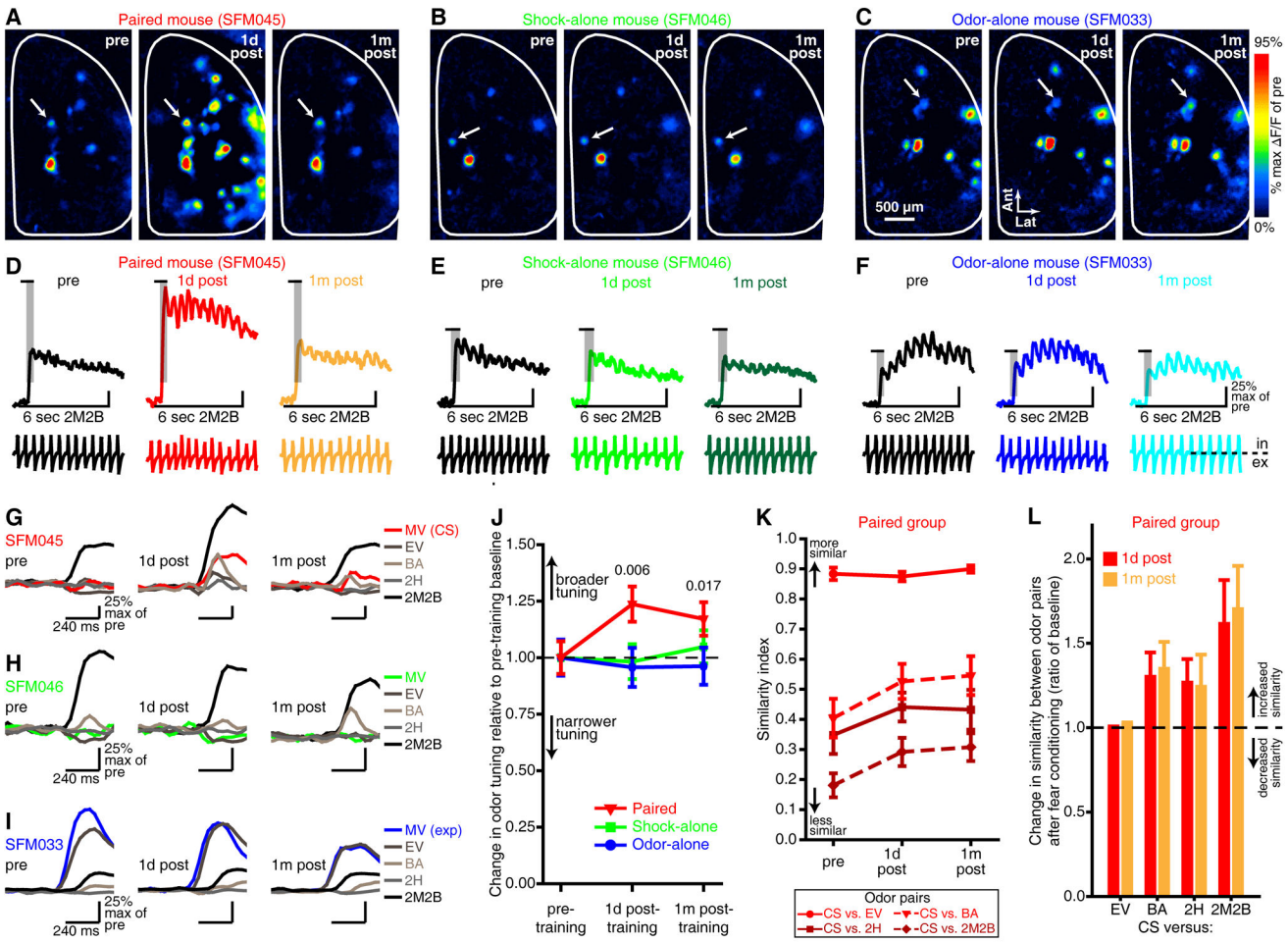

Figure 4. PG interneurons exhibit a decrease in odor response selectivity after olfactory fear conditioning with a single CS

(A–F) Difference maps **(A–C)** and corresponding fluorescence (top) and respiration (bottom) records **(D–F)** that were measured from single trials of 2M2B that were presented 1 day before (left, pre), 1 day after (middle, 1d post), and 1 month after (right, 1m post) each representative subject underwent either paired **(A,D)**, shock-alone **(B,E)**, or odor-alone **(C,F)** training. 2M2B was an unexposed odor for all 3 groups. The shaded regions on the response amplitudes in **D–F** indicate the frames corresponding with inhalation 1-evoked maps **(A–C)** and analyses **(J–L)**. Tick marks shown immediately above the shaded regions note the frames that are expanded in **G–I. (G–I)** Example odor response selectivity patterns across imaging sessions from the glomeruli in **A–F**. GCaMP signals that were evoked by the first inhalation of each of the other 4 odors in the panel were superimposed on the 2M2B-evoked amplitude from each imaging session for each glomerulus. **(J)** Odor-evoked activity in PG interneurons from paired mice exhibited a decrease in selectivity (broader tuning) relative to pre-training baseline (dashed line), while no change in selectivity was observed across imaging sessions in the shock-alone or odor-alone groups. *P* values are compared to pre-training baseline for paired mice. **(K–L)** After olfactory fear conditioning, PG cell activity maps that were evoked by unexposed odors tended to become slightly more similar

to the CS-evoked PG cell activity map, with the largest change in odor map similarity occurring between maps that were the least similar at baseline. **(K)** Mean±SEM similarity index between the CS and the other 4 unexposed odors across imaging sessions, where a value of 1 notes complete similarity between an odor pair and 0 notes complete dissimilarity between an odor pair. **(L)** Relative changes in similarity between the CS versus each of the other 4 unexposed odors 1 day and 1 month after training.

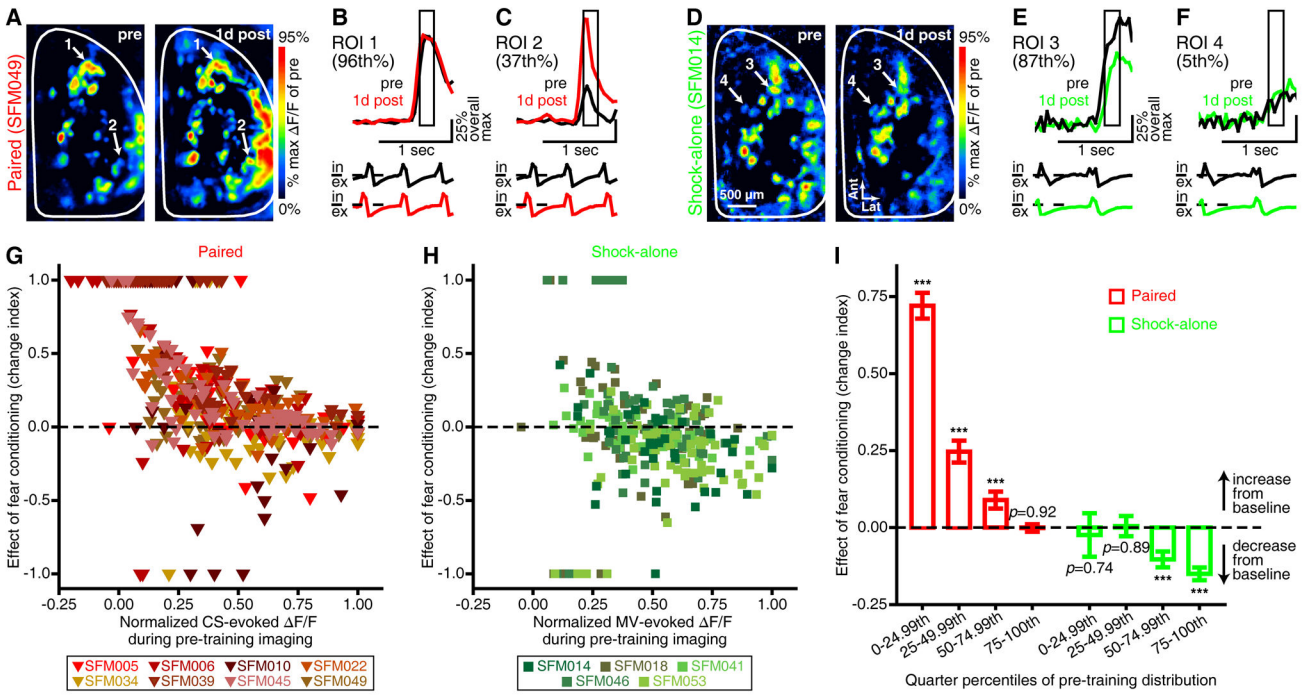

Figure 5. Fear conditioning-induced alterations in PG interneuron activity are dependent upon baseline response amplitudes

(A,D) Pseudocolored difference maps that were evoked by the CS 1 day before (pre, left) and 1 day after (1d post, right) either paired **(A)** or shock-alone **(D)** conditioning. Examples in **A–F** are from individual trials. These representative paired **(A–C)** and shock-alone **(D–F)** subjects respectively had 66 and 42 CS-responsive glomeruli (across both olfactory bulbs) that were rank-ordered from lowest to highest based on pre-training response amplitudes (ΔF/Fs). The sample traces show CS-evoked ΔF/Fs (top) in high-ranking (**B**, 96th percentile; **E**, 87th percentile) and low-ranking (**C**, 37th percentile; **F**, 5th percentile) glomeruli from 1 day before and 1 day after paired **(B,C)** or shock-alone **(E,F)** conditioning. ΔF/Fs are scaled relative to the overall max of pre-training across both ROIs per subject and are aligned relative to the first second of the CS (stimulus bar, middle) and the corresponding respiration records (bottom; in, inhalation; ex, exhalation). Boxed regions indicate inhalation 1-evoked difference maps **(A,D)** and analyses **(G–I). (G,H)** Scatterplots showing the changes in CS-evoked PG cell activity 1 day after paired (**G**, $N = 449$) or shock-alone (**H**, $N = 277$) conditioning (y-axes) relative to normalized pre-training response amplitudes (x-axes). Data points above and below the dashed lines respectively indicate increases and decreases from pre-training baseline. Each data point represents a single glomerulus, and all glomeruli from a given subject are color-coded per the keys. **(I)** Mean±SEM effect of paired (left, red) or shock-alone (right, green) conditioning 1 day after training for glomeruli that are grouped into quarter percentiles of the pre-training response distribution. Note that ***indicates $p <$ 0.001, and all P values are against pre-training baseline by one-sample t tests. Fear conditioning **(A,B,C,G,I)** enhanced PG cell activity more in glomeruli that exhibited the weakest CS-evoked responses during pre-training imaging, whereas shock-alone training

(D,E,F,H,I) reduced PG cell activity in glomeruli that exhibited the largest baseline responses to the CS (which was just an unexposed odor for this group).

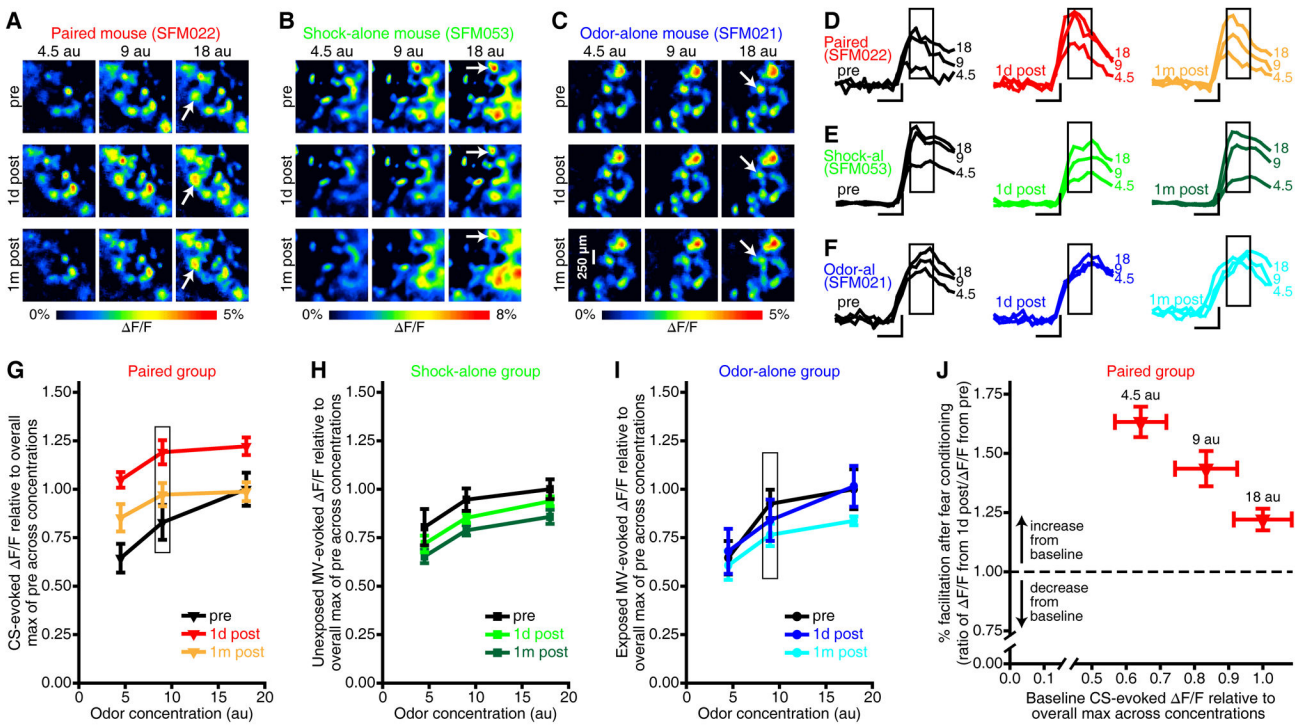

Figure 6. Enhanced sensitivity of PG interneurons after fear conditioning

(A–F) PG activity maps **(A–C)** and fluorescence records **(D–F)** from 1 day before, 1 day after, and 1 month after each representative subject underwent either paired **(A,D)**, shock-alone **(B,E)**, or odor-alone **(C,F)** training. Examples in **A–F** are from the first inhalation of odor during individual trials of each of 3 concentrations of MV, which was the CS for paired subjects, an unexposed ester for shock-alone subjects, and the exposed ester for odor-alone subjects. Traces for each ROI **(D–F)** are scaled relative to the overall max ΔF/F across concentrations from pre-training (scale bar: vertical, 25% overall max of pre; horizontal, 200 ms). Boxed regions note the frames corresponding with inhalation 1-evoked activity maps **(A–C)** and analyses **(G–J). (G–I)** The mean±SEM MV-evoked ΔF/F is plotted as a function of odor concentration (shown in arbitrary units, au) for each imaging session from paired **(G)**, shock-alone **(H)**, and odor-alone **(I)** groups. Boxed data points indicate the training concentration for paired and odor-alone groups. **(J)** Scatterplot showing the facilitation of CS-evoked PG cell activity 1 day after training (*y*-axis) relative to normalized baseline response amplitudes (*x*-axis) for each concentration of the CS. These data are pooled across 8 paired subjects and displayed as mean±SEM ΔF/F ratios (*y*-axis) and mean±SEM baseline ΔF/Fs (*x*-axis).